Energy 147 (2018) 578–586

Contents lists available at ScienceDirect

Energy

journal homepage: www.elsevier.com/locate/energy

A hybrid system using direct contact membrane distillation for water production to harvest waste heat from the proton exchange membrane fuel cell

Xiaotian Lai, Rui Long*, Zhichun Liu, Wei Liu**

School of Energy and Power Engineering, Huazhong University of Science and Technology, 1037 Luoyu Road, Wuhan 430074, China

ARTICLE INFO

Article history:
Received 10 July 2017
Received in revised form
9 January 2018
Accepted 18 January 2018
Available online 18 January 2018

Keywords:
Proton exchange membrane fuel cell
Direct contact membrane distillation
Waste heat recovery

ABSTRACT

In this paper, a hybrid system consisting of PEMFC (proton exchange membrane fuel cell) and DCMD (direct contact membrane distillation) was proposed to recover the waste heat from PEMFC for brine water desalination. Parameters determining the performance of this hybrid system were systematically investigated. Results indicate that there exist optimal PEMFC current density and DCMD fresh water inlet mass flow rate, respectively, leading to the maximum energy gain from the fuel chemical energy. In order to analyze the optimal performance of the proposed hybrid system, with the maximum energy gain as the objective function, genetic algorithm method was employed to obtain the optimal PEMFC current density and DCMD fresh solution inlet mass flow rate, thereby, the performance specifications of the hybrid system under different operating temperatures of the PEMFC subsystem. Compared with the single PEMFC system, as operating temperature varies from 328.15 K to 348.15 K, the energy utilization degree can be increased by 201%–266%.

1. Introduction

Rapid increase of population and fast industrialization call for dramatically increasing energy supply and water consumption. Combustion of conventional fossil fuels have caused serious catastrophe to the environment, such as global warming and animal annihilation [1]. Hence, optimizing the conventional thermodynamic cycles and developing clean and sustainable energy technologies is becoming more and more urgent [2–5]. Among them, fuel cells which convert chemical energy into electricity directly are regarded as a prospective way to solve these severe problems.

Common fuel cells can be classified into five categories: alkaline fuel cell (AFC), phosphoric acid fuel cell (PAFC), proton exchange membrane fuel cell (PEMFC), molten carbonate fuel cell (MCFC) and solid oxide fuel cell (SOFC) [6]. Compared to other fuel cells, PEMFC has several predominant features such as clean production (water), high power density and rapid start up time. These superiorities made it widely used in automotive and residential applications [6–11]. It is noteworthy that during the reaction of PEMFC, electricity is obtained meanwhile considerable heat is produced [12,13]. To keep stable operation, the heat exhausted by PEMFC needs to be released into a heat sink. Hence, the energy utilization degree of PEMFC is generally around 50% conditioned on the companied heat generation. For further utilizing the heat generated by PEMFC, various waste heat recovery technologies have been investigated numerically and experimentally. One of the methods is to improve the electrical power output by employing low-temperature power generation technologies [6,8,11,14]. Dai et al. [8] proposed a hybrid system using ORC (organic Rankine cycle) to harvest waste heat from PEMFC. The results show that the total electrical efficiency is increased by around 5%. Chen et al. [11] employed a thermoelectric generator to convert the waste heat into electricity. Their research indicates the maximal electrical power output raised around 9%. R. Long et al. [14] proposed a similar hybrid system which utilizes TREC (thermally regenerative electrochemical cycle) as the waste heat harvesting section for PEMFC and made the efficiency increased by 6.85%–20.59%. In addition to utilizing the waste heat to generate electricity, the PEMFC-based CHP (combined heat and power) system is also an effective method to improve energy utilization degree in residential application [7,15,16]. Barelli et al. [7] made a research on a system which utilizes waste heat recovered

* Corresponding author.
** Corresponding author.
E-mail addresses: r_long@hust.edu.cn (R. Long), w_liu@hust.edu.cn (W. Liu).

https://doi.org/10.1016/j.energy.2018.01.065
0360-5442/

from PEMFC for heating water, and this system is able to satisfy the residential demand of electricity and heat water simultaneously. The energy utilization degree increases from 34% to 92%. Arsalis et al. [15] proposed a HT (high temperature)-PEMFC-based micro CHP system for a Danish single-family household. In their research, with the load fully applied, electrical efficiency is 38.8% but corresponding total energy utilization degree is promoted to around 95.2%. In terms of energy utilization degree, direct use of waste heat of PEMFC is more competitive. In recent decades, with rapid increasing of fresh water consumption, low-temperature driven water treatment technology has become an effective waste heat harvesting method as well [17–25]. Thermal type water treatment method mainly includes MSF (multi-stage flash), MED (multi-effect distillation) and DCMD (direct contact membrane distillation) [21,23,24,26,27]. Considering the advantages of low complexity and operating temperature [28,29], DCMD is more suitable to ally with PEMFC, serving as an electricity and fresh water supplier for coastal residential application. Until now, relevant research has not been reported yet.

DCMD [19,26,27] is a separation technic which utilizes the difference of vapor partial pressure originating from the temperature difference of hot brine water and cool fresh water as driving force. During the separation process, hot brine water flows into brine side channel at first. Then due to the vapor partial pressure difference and hydrophobic nature of the membrane, hot water gets vapored and transferred into cool fresh side. Finally, hot vapor gets condensed at cool fresh side while mixing with fresh water. As mentioned above, the operating temperature of DCMD is low, always around 40°C-70 °C. It means DCMD can play an important role in low temperature waste harvesting area. Duke et al. [30] conducted a pilot DCMD trial for treatment of power station waste water driven by the waste heat of 38 °C from power station. Over three months of the operation, high water recovery (92.8%) and quality of distillate production (with 99.9% dissolved solids rejected) were achieved. Vidic et al. [17] employed DCMD to utilize the waste heat from NG CS (natural gas compressor station) in Pennsylvania, United States for concentration. Their research indicates that, with numerous amount of waste heat from NG CS, the outlet water flow with 30% salinity can be sufficiently produced regardless of the initial salinity. Boubakri et al. [29] designed a pilot DCMD system driven by solar energy and tested its performance. The results indicates that powered by solar energy, the inlet temperature of feed flow could be elevated to around 70 °C. Minimum specific energy consumption of 1609 kWh/m^3 during 12:30–13:00 (under maximal sunlight intensity) was achieved.

In summary, low complexity makes the integration of DCMD and PEMFC prospective for residential application in coastal region. Besides, the operating temperature of PEMFC is generally set between 70°C and 90 °C [8,11,14], which exactly satisfies the inlet temperature requirement of feed flow in DCMD. Thereby a hybrid DCMD system coupled with PEMFC is proposed for electricity supply and fresh water production in this paper. This system outputs electricity and fresh water simultaneously at the cost of consuming hydrogen. Compared with a single PEMFC system, with the waste heat recovered, the energy utilization degree augments significantly. In order to investigate the performance of this system, mathematical models of the hybrid system were set up, and impacts of PEMFC current density [31,32] and fresh water inlet mass flow rate of DCMD [29,33] on the performance of the hybrid system and its subsystems are discussed. The results indicate there exit optimal current density and inlet mass flow of fresh water for the maximal energy gain of the hybrid system. Hence, an optimization based on genetic algorithm is conducted with the maximum energy gain as the objective function. The optimal performance specifications of the hybrid system and its subsystems have been obtained under different operating temperature of the PEMFC and initial concentration of brine water. Finally, some concluding remarks are presented.

2. System description and mathematical model

2.1. System description

As shown in Fig. 1, this hybrid system consists of two main components: PEMFC for electricity generation and DCMD for fresh water production. In the PEMFC, hydrogen and oxygen are fed into corresponding channel where the electrochemical reaction happens. During the reaction, electricity is generated meanwhile heat is produced. The waste heat is applied to elevate the inlet temperature of brine water. In DCMD, driven by the partial vapor pressure difference originating from the temperature difference of brine and fresh water, a transmembrane vapor flux happens. Hot water evaporates at brine water side, diffuses into fresh water side, and gets condensed while mixing with cool fresh water. Then fresh water flows into a separator for condensed water extraction. Finally, remaining fresh water is cooled by a heat sink and fed into DCMD as permeate solution again. Furthermore, to improve the energy efficiency of the DCMD system, a regenerator is utilized to preheat the brine water before absorbing heat released from PEMFC [34].

2.2. Mathematical model

2.2.1. PEMFC

In the PEMFC, hydrogen and oxygen are fed into their corresponding channel and react as follows:

$$\text{Anode}: \ H_2 \rightarrow 2H^+ + 2e^-$$

$$\text{Cathode}: O_2 + 4H^+ + 4e^- \rightarrow 2H_2O$$

According to Nernst equation [35], the voltage can be expressed as

$$V_{Nernst} = 1.229 - 0.85 \times 10^{-3}(T - 298.15) + 4.3085 \times 10^{-5} T\left[\ln(P_{H_2}) + 0.5\ln(P_{O_2})\right] \quad (1)$$

where T is the operating temperature of PEMFC. p_{H_2} and p_{O_2} is the partial pressure of hydrogen and oxygen respectively which can be derived from the following equations [36] in sequence:

$$\log_{10}\left(p_{H_2O}^{sat}\right) = -2.1794 + 0.02953(T - 273.15) - 9.1837 \times 10^{-5}(T - 273.15)^2 + 1.4454 \times 10^{-7}(T - 273.15)^3 \quad (2)$$

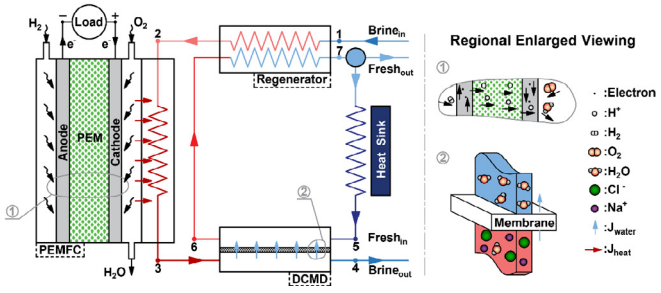

Fig. 1. Schematic diagram of the hybrid PEMFC-DCMD system.

$$x_{H_2O}^{sat} = \frac{p_{H_2O}^{sat}}{p} \tag{3}$$

$$p_{H_2} = 0.5 p_{H_2O}^{sat} \frac{1}{e^{\frac{4.192j}{T^{1.334}}} x_{H_2O}^{sat}} - 1 \tag{4}$$

$$p_{O_2} = p_{H_2O}^{sat} \frac{1}{e^{\frac{4.192j}{T^{1.334}}} x_{H_2O}^{sat}} - 1 \tag{5}$$

where $p_{H_2O}^{sat}$ is the saturation pressure of water, p is the operating pressure of PEMFC. But in reality, when PEMFC operates, there are three kinds of voltage losses existing. The ohmic loss V_{oh}, activation loss V_{act} and concentration loss V_{con} can be derived by following equations [8,13],:

$$V_{oh} = \frac{181.6j\left[1 + 0.03j + 0.62\left(\frac{T}{303}\right)^2 j^{2.5} L_1\right]}{(14 - 0.634 - 3j)e^{4.18\left(1-\frac{303}{T}\right)}} \tag{6}$$

$$V_{act} = 0.9514 - 0.00312T - 0.000074T \ln\left(1.97 \times 10^{-7} p_{O_2} e^{\frac{489}{T}}\right) + 0.000187T \ln(jA) \tag{7}$$

$$V_{con} = 4.3085 \times 10^{-5} T \ln\left(\frac{j_l}{j_l - j}\right) \tag{8}$$

where L_1 represents the thickness of membrane, j_l is limiting current density. The real total voltage V_{total} is:

$$V_{total} = V_{Nernst} - V_{oh} - V_{act} - V_{con}. \tag{9}$$

Then the electricity output of PEMFC P_{PEMFC} is given by

$$P_{PEMFC} = N_{fc} V_{total} jA \tag{10}$$

Here, we express the total energy input $\dot{Q}_{total}$ as:

$$\dot{Q}_{total} = N_{fc} \frac{jA}{2F} HHV \tag{11}$$

where N_{fc} is the number of fuel cells, j is current density, A is the effective area of PEMFC, F is Faraday constant, and HHV is the high heating value of hydrogen. Therefore, the electrical efficiency of the PEMFC is

$$\eta_{PEMFC} = \frac{P_{PEMFC}}{\dot{Q}_{total}}. \tag{12}$$

Meanwhile heat released by the PEMFC $\dot{Q}_{re}$ can be calculated by:

$$\dot{Q}_{re} = N_{fc} jA(V_{oh} + V_{act} + V_{con}) + N_{fc} \frac{jA}{2F}(HHV - 2FV_{Nernst}). \tag{13}$$

2.2.2. DCMD

In the DCMD, mass transfer and heat transfer occur simultaneously. Though real heat transfer consists of convective heat transfer originating from mass transfer of vapor and conductive heat transfer originating from the conductivity of membrane, for simplicity, conductive transfer is neglected. Hence, mass and heat transfer processes can be expressed as:

$$\frac{d\dot{m}_B(x)}{dx} = w_{DCMD} K_{m,DCMD}(T_B(x) - T_F(x) - \Delta T_{th}(x)) \tag{14}$$

$$\frac{d\dot{m}_F(x)}{dx} = w_{DCMD} K_{m,DCMD}(T_B(x) - T_F(x) - \Delta T_{th}(x)) \tag{15}$$

$$\frac{d\left[\dot{m}_B(x) h_{liq}(C(x), T_B(x))\right]}{dx} = \frac{d\dot{m}_B(x)}{dx}\left[h_{vap}(C(x), T_B(x)) + h_{liq}(0, T_B(x))\right] \tag{16}$$

$$\frac{d\left[\dot{m}_F(x) h_{liq}(0, T_F(x))\right]}{dx} = \frac{d\dot{m}_F(x)}{dx}\left[h_{vap}(0, T_F(x)) + h_{liq}(0, T_F(x)) + c_{p,vap}(T_B(x) - T_F(x))\right] \tag{17}$$

where $\dot{m}_B(x)$, $\dot{m}_F(x)$, $T_B(x)$, $T_F(x)$ represent mass flow rate, temperature of brine water and fresh water at any point along the length of DCMD. $\Delta T_{th}(x)$ is threshold temperature difference that means only when temperature difference between two sides is greater than it, vapor transfer occurs. $h_{liq}(C(x), T_B(x))$ and $h_{vap}(C(x), T_B(x))$ represent the enthalpy of brine water ($C(x) = 0$ means fresh water) and evaporation process under any concentration and temperature. $c_{p,vap}$ is the specific heat of vapor. w_{DCMD} and $K_{m,DCMD}$ are width and mass transfer coefficient of DCMD. The temperature and mass flow rate distributions can be calculated based on Eqs. (14)–(17) with the boundary conditions listed below:

$$T_B(L) = T_3 \tag{18}$$

$$T_F(0) = T_5 \tag{19}$$

$$\dot{m}_B(L) = \dot{m}_1 \tag{20}$$

$$\dot{m}_F(0) = \dot{m}_5. \tag{21}$$

To improve the energy efficiency of the DCMD system, a regenerator is applied to preheat the brine water before absorbing heat released from the PEMFC. The differential equations below can be established [37].

$$\frac{dT_{Reg\_B}(x)}{dx} = \frac{w_{Reg} K_{Reg}\left(T_{Reg\_F}(x) - T_{Reg\_B}(x)\right)}{\dot{m}_1 c_p\left(T_{Reg\_B}(x), C(x)\right)} \tag{22}$$

$$\frac{dT_{Reg\_F}(x)}{dx} = \frac{w_{Reg} K_{Reg}\left(T_{Reg\_F}(x) - T_{Reg\_B}(x)\right)}{\dot{m}_6 c_p\left(T_{Reg\_F}(x), 0\right)} \tag{23}$$

where K_{Reg} is the heat transfer coefficient of regenerator, w_{Reg} is the width of heat transfer surface. $T_{Reg\_B}(x)$, $T_{Reg\_F}(x)$, $c_p(x, C(x))$, $c_p(x, 0)$ are temperature, specific heat of brine water and fresh water at any point x along the length of heat transfer surface respectively. $C(x)$ is the concentration of brine water at any point x along the length of heat transfer surface. $\dot{m}_1$, $\dot{m}_6$ are mass flow rate of brine water and fresh water respectively. The temperature distribution can be calculated based on Eqs. (22) and (23) with the boundary conditions given by:

$$T_{Reg\_B}(0) = T_1 \tag{24}$$

$$T_{Reg\_F}(0) = T_7. \tag{25}$$

For brine water heater, the heat absorbed from the PEMFC can be expressed as:

$$\dot{Q}_{DCMD} = \dot{m}_1 (T_3 c_p(T_3, C_1) - T_2 c_p(T_2, C_1)) \quad (26)$$

where T_2, T_3, $c_p(T_2, C_1)$, $c_p(T_3, C_1)$ are temperature, specific heat at inlet and outlet of brine water heater separately.

According to aforementioned equations, the performance evaluation parameters ε (fresh water production rate) and the *GOR* (gain output ratio) of DCMD can be derived by:

$$\varepsilon = \frac{\Delta m_w}{\dot{m}_3} \quad (27)$$

$$GOR = \frac{\Delta m_w \Delta H_v}{\dot{Q}_{DCMD}} \quad (28)$$

where $\dot{m}_3$ is the inlet mass flow rate of brine water, Δm_w is the mass flow rate of transmembrane water in the DCMD device, ΔH_v is the evaporation enthalpy. As the Eqs. (27) and (28) expressed, ε represents the relative ability of fresh water producing and *GOR* represents the ratio of benefit and consumption in the DCMD process.

2.3. Overall energy utilization degree of the hybrid PEMFC-DCMD system

The proposed PEMFC-DCMD system consumes the chemical energy of the hydrogen in the PEMFC and generates electricity as well as fresh water. The overall energy utilization degree, ζ, can be defined as:

$$\zeta = \frac{P_{ele} + \Delta m_w \Delta H_v}{\dot{Q}_{total}} = \frac{E_{hybrid}}{\dot{Q}_{total}} \quad (29)$$

In order to evaluate the performance of the hybrid system with the same dimension, $E_{hybrid} = P_{ele} + \Delta m_w \Delta H_v$ is defined as the energy gain of the hybrid system.

3. Results and analysis

3.1. Sensitivity analysis of the hybrid PEMFC-DCMD system

Based on the mathematical model set above, we investigated the influence of operating parameters on the performance in this part of work. The past researches indicate the current density influences the power generation and heat release of PEMFC significantly [31,32]. Thereby, the change of heat supply from the upstream (PEMFC) will affect the performance of DCMD naturally. In the downstream (DCMD), the fresh water production relies on the inlet mass flow rate of brine and fresh solution strongly [29,33]. Therefore, a sensitivity analysis should be carried to investigate the impacts of these parameters on the overall performance of the proposed hybrid system. The prescribed variables for the mathematical model of the hybrid system are shown in Table 1.

Fig. 2 shows the relation of energy output of the hybrid system and subsystems with current density of the PEMFC subsystem. Power generated by the PEMFC increases with increasing current density first, reaches its maximum value, then decreases. As current density changes from 0.6 A/cm^2 to 1.38 A/cm^2, electrical power increases from 43 kW to 75 kW. It can be seen that as the current density is larger than 1.38 A/cm^2, the increase of the current density cannot atone for the decrease of the voltage, which leads a decrease of electrical power. As depicted in Fig. 2, heat recovered from PEMFC, which equals to the heat absorbed by the DCMD device, $\dot{Q}_{DCMD}$, increases with increasing PEMFC current density. When current density increases from 0.6 A/cm^2 to 1.48 A/cm^2, $\dot{Q}_{DCMD}$ increases from 77 kW to 88 kW. The increment of current density leads to the increment of voltage losses, and more heat supplies for DCMD. The energy gain (E_{Hybrid}) of the hybrid system is the sum of recovered heat carried by the transmembrane water and electricity output, which presents a similar trend with electrical power. E_{Hybrid} increases with increasing current density first, reaches its maximum value, then decreases.

Table 1
Parameters setting for calculation.

Parameter	Abbreviation	Unit	Value
Number of fuel cells	N_{fc}		300
Effective area of PEMFC	A	cm^2	300
Current density of PEMFC	j	A/cm^2	1.2
Limiting current density of PEMFC	j_l	A/cm^2	1.5
Thickness of PEM	L_1	cm	0.00254
Faraday constant	F	C/mole	96485
Temperature of PEMFC	T_{PEMFC}	K	333.15
Pinch point of brine water heater	ΔT	K	4
Inlet temperature of fresh water	T_5	K	293.15
Inlet mass flow rate of fresh water	$\dot{m}_5$	kg/s	0.9
Width of DCMD	w_{DCMD}	m	8
Length of DCMD	L_{DCMD}	m	2
Inlet concentration of brine water	$C(L)$	mole/kg	3
Mass transfer coefficient of DCMD	$K_{m,DCMD}$	kg/(m^2 s C)	0.0005
Thickness of hydrophobic membrane	L_2	m	0.0001
Heat transfer coefficient of regenerator	K_{Reg}	w/(m^2·K)	1000
Width of regenerator	w_{Reg}	m	6
Length of regenerator	L_{Reg}	m	4

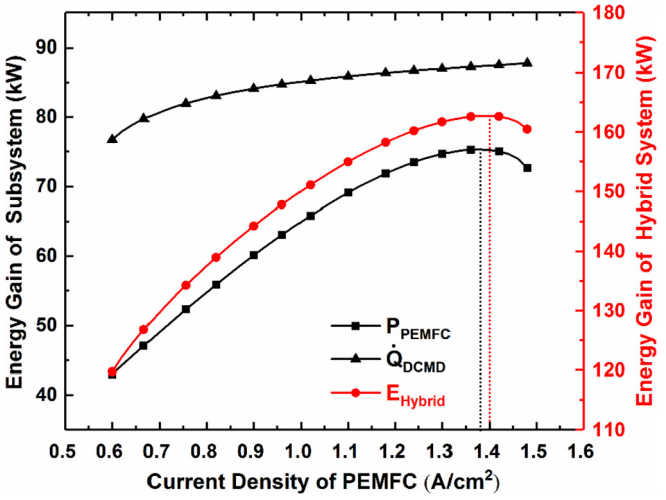

Fig. 2. Energy gain of the hybrid system and subsystems as a function with current density.

Fig. 3 illustrates the relationship between efficiency and energy utilization degree with current density, respectively. It can be seen that as current density increases from 0.6 A/cm^2 to 1.48 A/cm^2, electrical efficiency decreases from 54% to 37% due to the increment of voltage loss. Meanwhile, *GOR* decreases from 2.09 to 0.71. Although the heat supplying for DCMD increases with the increment of current density, heat recovery ability is limited because the inlet mass flow rate of cool fresh water is kept constant here, which leads to the decrement of *GOR*. Energy utilization degree of the hybrid system ζ decreases from 1.50 to 0.82 as current density changes from 0.6 A/cm^2 to 1.48 A/cm^2.

Fig. 4 shows that as current density increases from 0.6 A/cm^2 to 1.48 A/cm^2, inlet and outlet mass flow rate of brine water increases

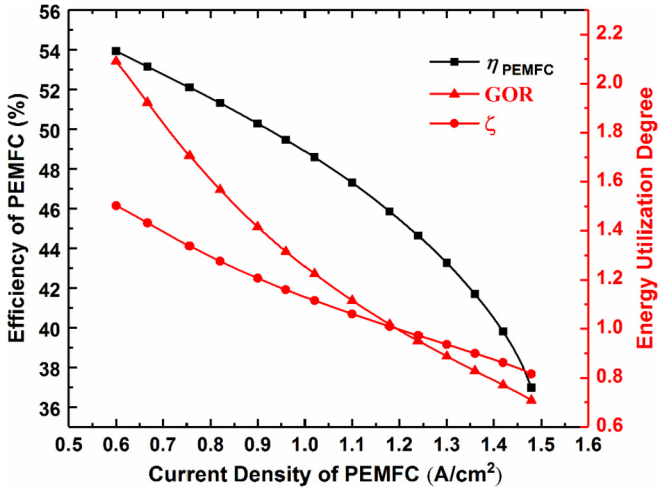

Fig. 3. Efficiency and energy utilization degree of hybrid system and subsystems as a function with current density.

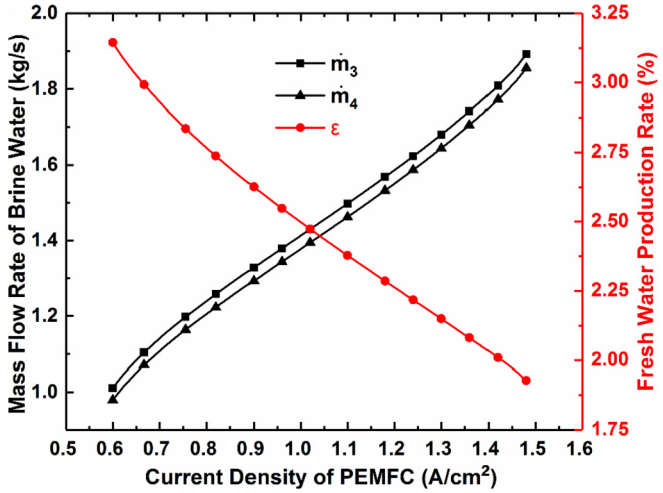

Fig. 4. Mass flow rate of brine water and fresh water production rate as a function with current density.

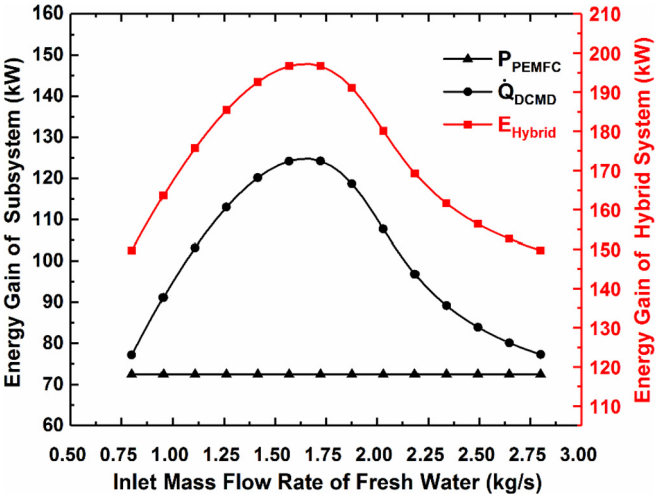

Fig. 5. Energy gain of hybrid system and subsystems as a function with inlet mass flow rate of fresh water.

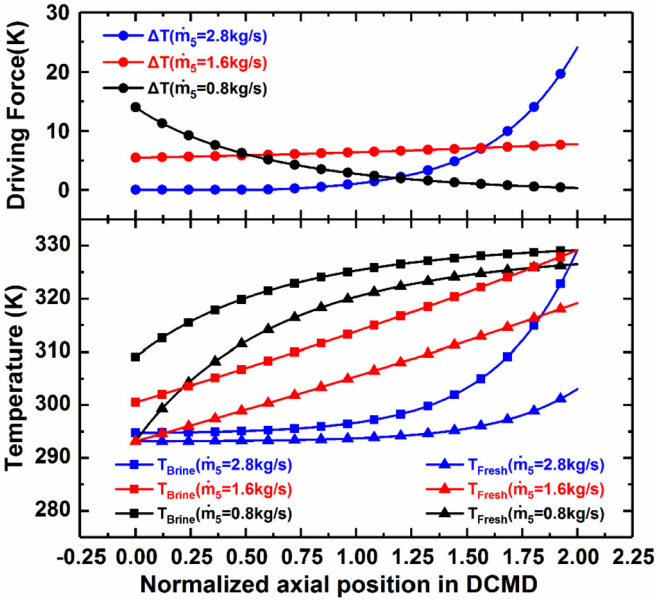

Fig. 6. Distributions for temperature and transfer driving force along the length of DCMD.

from 1.04 kg/s to 1.93 kg/s, 1.01 kg/s to 1.89 kg/s respectively. The increment of heat released from PEMFC needs to be taken away by more brine water to keep the temperature of PEMFC constant. However, the fresh water production rate decreases with the increment of current density conditioned on the limited membrane area of the DCMD device. From Fig. 4, it can be seen that the curves of inlet mass flow rate and outlet mass flow rate are nearly parallel. That is to say the mass flow rate of vapor nearly stays constant with the increment of current density which leads the decrease of fresh water production rate.

As depicted in Fig. 5, the fresh water mass flow rate in the DCMD only influences the performance of the downstream DCMD and has no effects on the energy output of the upstream PEMFC. Electrical power generated in PEMFC keeps constant as the mass flow rate increases from 0.8 kg/s to 2.8 kg/s. Meanwhile, the mass flow rate increases from 0.8 kg/s to 1.6 kg/s, and the heat recovered increases from 77 kW to 125 kW. As the mass flow rate is larger than 1.6 kg/s, the heat recovered begins to decrease. Fig. 6 illustrates the temperature and transfer driving force along the length of DCMD which can explain the phenomenon above. It can be seen that when the mass flow rate reaches 1.6 kg/s which leads to the maximum of recovered heat, the transfer driving force along the length of DCMD only changes slightly and keeps a relatively high average value. However, as the mass flow rate deviates from 1.6 kg/s, transfer driving force changes significantly along the length of DCMD and has lower average value, which leads to the decrease of heat recovered. The energy gain of hybrid system shows the same trend with the heat recovered. When mass flow rate changes from 0.8 kg/s to 1.6 kg/s, energy gain of the hybrid system increases from 149 kW to the maximum value which is 197 kW, and then decreases.

As shown in Fig. 7, when the inlet mass flow rate of fresh water increases from 0.8 to 2.8 kg/s, mass transfer flow rate of vapor increases to the maximum value that is around 0.052 kg/s then decreases gradually. The fresh water production rate increases with increment of the inlet mass flow rate of fresh water nearly linearly at low values of the inlet mass flow rate. When the mass flow rate is larger than 2.1 kg/s, the fresh water production rate increases much

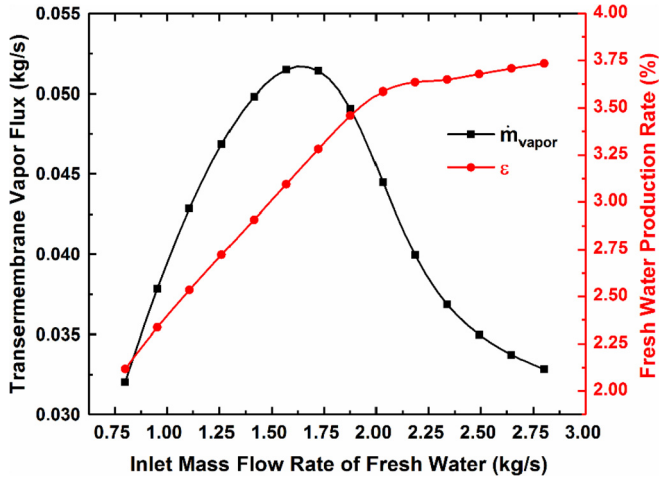

Fig. 7. Transmembrane vapor flux and fresh water production rate as a function with the inlet mass flow rate of fresh water.

more slowly. As the energy gain carried by the water vapor in the DCMD relies on the transmembrane vapor flux, the GOR present the same trend with the transmembrane vapor flux as shown in Fig. 8. Energy utilization degree and *GOR* increase as inlet mass flow rate of fresh water increases at first, reach their maximum value at 1.6 kg/s, then decrease. Furthermore, it can be seen that the increment of inlet mass flow rate of fresh water has no effect on electrical efficiency.

3.2. Maximum energy gain of the hybrid PEMFC-DCMD system

According to the results in sensitivity analysis, there exist optimal current density of PEMFC and fresh water mass flow rate of DCMD leading to the maximum energy gain of hybrid system respectively. For achieving the maximal energy gain of the hybrid system, GA (genetic algorithm) is employed to obtain the optimal parameters with the maximal energy gain as the objective function. GAs are a series of methods which are based on the process of natural selection. Due to the advantage of being able to solve complex optimization problems such as multi-parameter and multi-objective optimization problems, GAs have been widely used

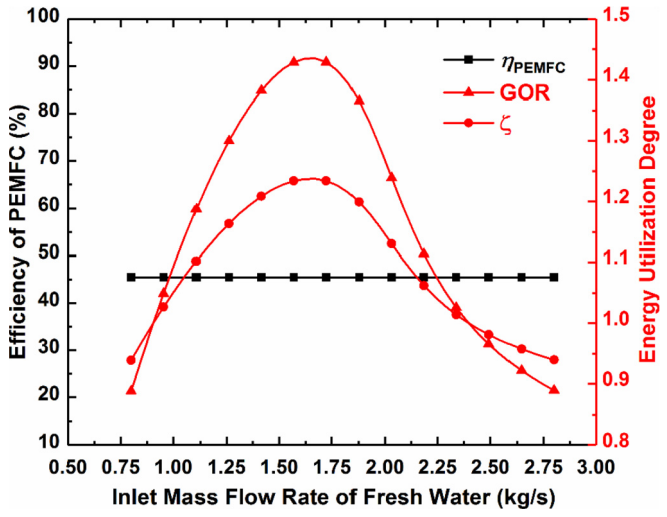

Fig. 8. Efficiency and energy utilization degree of hybrid system and subsystems as a function with the inlet mass flow rate of fresh water.

in many optimization areas [14,38–42]. R. Long et al. [14] used GAs to find the optimal current densities of two subsystems for achieving the maximum power of a PEMFC-TREC hybrid system. Zhi-Jun Mo et al. [39] used a method called niche genetic algorithm for parameter determination and optimization of PEMFC. Based on GA, with the maximum energy gain as the objective function, the corresponding energy gain and energy utilization degree of the hybrid system and its subsystems under different operating temperatures and different concentrations (1 mol/kg, 3 mol/kg) were obtained.

As illustrated in Fig. 9 (a), optimal power generated in PEMFC increases with increasing PEMFC operating temperature. When temperature is 328.15 K, electrical power is around 71 kW, which increases to around 74 kW at 348.15 K. The concentration of brine water has nearly no influence on the electrical power. The variation of PEMFC operating temperature and concentration of brine water are both able to influence the energy gain of DCMD. The heat recovered of DCMD under optimal condition increases with increasing PEMFC operating temperature. When temperature is 328.15 K and concentration is 3 mol/kg, transmembrane vapor flux is 209 kg/h and the energy gain of DCMD is 141 kW. As temperature gets to 348.15 K and concentration decreases to 1 mol/kg, transmembrane vapor flux is 298 kg/h and heat recovered by DCMD can be increased to 198 kW, as shown in Fig. 9 (b) and (d). In Fig. 9 (c), when temperature is 328.15 K and concentration is 3 mol/kg, energy gain of the hybrid system is 211 kW. As the PEMFC temperature increases to 348.15 K and concentration decreases to 1 mol/kg, energy gain of the hybrid system is 272 kW. Higher operating temperature of PEMFC and lower concentration of brine water contribute to lager optimal energy gain of the hybrid system.

Fig. 10 indicates the energy utilization degree under the optimal conditions at different PEMFC operating temperatures and concentrations of brine water. Energy utilization degree of the hybrid system and its subsystems with temperature and concentration exhibits the same behavior with the energy gain. As depicted in Fig. 10 (a) when temperature is 328.15 K, electrical efficiency of the PEMFC is 35%. As temperature is increased to 348.15 K, electrical efficiency is 37.6%. In Fig. 10 (b), when temperature is 328.15 K and concentration is 3 mol/kg, *GOR* of DCMD is 1.10. As temperature increases to 348.15 K and concentration reaches 1 mol/kg, *GOR* of DCMD reaches 1.60. For the hybrid system, when temperature is 328.15 K and concentration is 3 mol/kg, energy utilization degree is 1.06. As temperature increases to 348.15 K and concentration decreases to 1 mol/kg, energy utilization degree of the hybrid system achieves 1.37, as shown in Fig. 10 (c). Compared to the efficiency of a single PEMFC system, energy utilization degree of the hybrid system is improved by 266% at 348.15 K.

4. Conclusion

In order to harvest the waste heat from PEMFC and improve energy utilization degree, a PEMFC coupled with DCMD hybrid system which outputs electricity and fresh water was proposed in this paper. Noticing the low complexity of construction and good linkage of operating temperature, we find there probably exists some value to integrate these two systems for residential application in the coastal region. To evaluate the performance of this hybrid system in depth, the impacts of PEMFC current density and fresh water mass flow rate on system energy gain, energy utilization degree and fresh water production rate were investigated numerically. The results revealed that the current density and fresh water mass flow rate can lead to the maximal energy gain, respectively. Thereby, the following optimization work was conducted with GA method. We find under the optimal condition, high

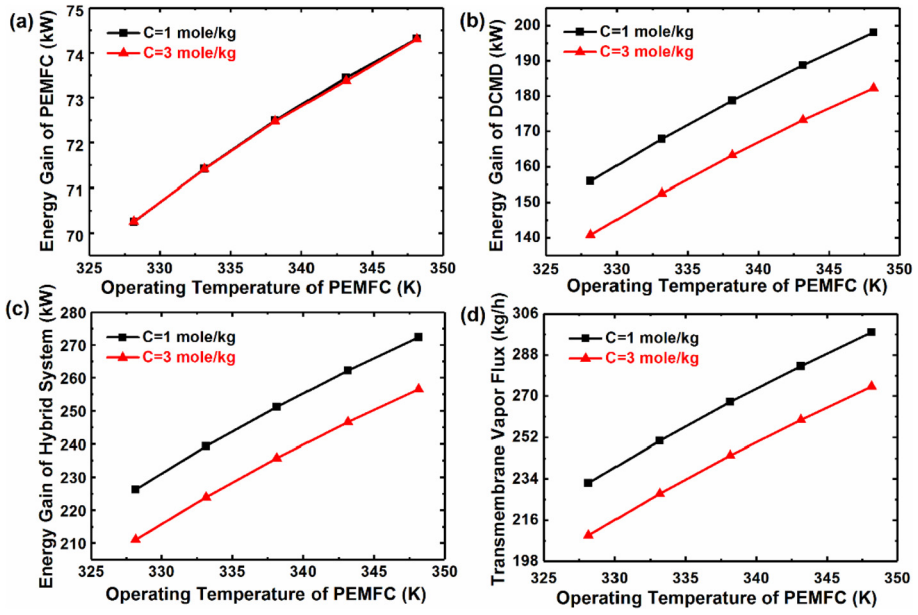

Fig. 9. Energy gain and transmembrane vapor flux under the optimal conditions at different temperature and concentration.

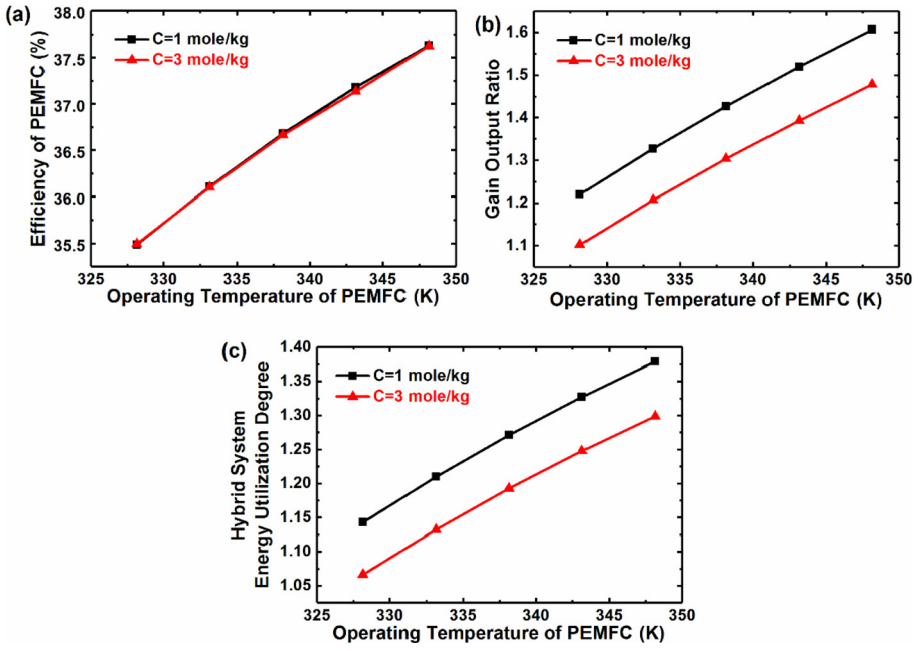

Fig. 10. Energy utilization degree under the optimal conditions at different temperature and concentration.

operating temperature of PEMFC and low initial concentration of brine water were beneficial to achieve better energy gain and energy utilization degree of this hybrid system. In summary, compared with a single PEMFC system, the energy utilization degree was increased by 201%–266% under maximal energy gain condition.

Acknowledgements

We acknowledge the support received from the National Natural Science Foundation of China (51706076, 51736004).

Nomenclature

$\dot{Q}_{total}$	Total energy input kW
N_{fc}	Number of fuel cells
j	Current density A/cm^2
A	Effective area of PEMFC cm^2
V_{Nernst}	Voltage according to Nernst equation V
T	Operating temperature of PEMFC K
p_{H_2}	Partial pressure of hydrogen Pa
p_{O_2}	Partial pressure of oxygen Pa
$p^{sat}_{H_2O}$	Saturation pressure of water Pa
p	Operating pressure of PEMFC Pa

V_{oh}	Ohmic voltage loss V
V_{act}	Activation voltage loss V
V_{con}	Concentration voltage loss V
V_{total}	Real total voltage V
P_{PEMFC}	Electricity output of PEMFC kW
η_{PEMFC}	Electrical efficiency %
$\dot{Q}_{re}$	Heat released by the PEMFC kW
K_{Reg}	Heat transfer coefficient of regenerator $\mathrm{w}/(\mathrm{m}^2\cdot\mathrm{K})$
w_{Reg}	Width of heat transfer surface in regenerator m
T_{Reg_B}	Temperature of brine water in regenerator K
T_{Reg_F}	Temperature of fresh water in regenerator K
$c_p(x, C(x))$	Specific heat of brine water $\mathrm{kJ}/(\mathrm{kg}\cdot\mathrm{K})$
$c_p(x, 0)$	Specific heat of fresh water $\mathrm{kJ}/(\mathrm{kg}\cdot\mathrm{K})$
$C(x)$	Concentration of brine water mole/kg
$\dot{m}_B$	Mass flow rate of brine water kg/s
$\dot{m}_F$	Mass flow rate of fresh water kg/s
T_B	Temperature of brine water in DCMD K
T_F	Temperature of fresh water in DCMD K
ΔT_{th}	Threshold temperature difference K
h_{liq}	Enthalpy of brine water kJ/kg
h_{vap}	Enthalpy of vapor kJ/kg
$c_{p,vap}$	Specific heat of vapor $\mathrm{kJ}/(\mathrm{kg}\cdot\mathrm{K})$
w_{DCMD}	Width of DCMD m
$K_{m,DCMD}$	Mass transfer coefficient of DCMD $\mathrm{kg}/(\mathrm{m}^2\cdot\mathrm{s}\cdot\mathrm{K})$
$\dot{Q}_{DCMD}$	Heat recovered by DCMD kW
E_{Hybrid}	Output of the hybrid system kW
ζ	Energy utilization degree of the hybrid system
Δm_w	Transmembrane water in the DCMD device kg/s

Greek Symbols

ζ	Energy utilization degree
η	Energy efficiency %
ε	Fresh water production rate %

Subscripts

Reg	Heat regenerator
B	Brine water
F	Fresh water
1–7	States in the system

Abbreviations

PEMFC	Proton exchange membrane fuel cell
DCMD	Direct contact membrane distillation
AFC	Alkaline fuel cell
PAFC	Phosphoric acid fuel cell
MCFC	Molten carbonate fuel cell
SOFC	Solid oxide fuel cell
NS CS	Natural gas compressor station
CHP	Combined heat and power
ORC	Organic Rankine cycle
TREC	Thermally regenerative electrochemical cycle
RO	Reverse osmosis
MSF	Multi-stage flash
MED	Multi-effect distillation
GOR	Gain output ratio
HHV	High heating value
GAs	Genetic algorithms

References

[1] Long R, Bao YJ, Huang XM, Liu W. Exergy analysis and working fluid selection of organic Rankine cycle for low grade waste heat recovery. Energy 2014;73:475–83.

[2] Long R, Li B, Liu Z, Liu W. Hybrid membrane distillation-reverse electrodialysis electricity generation system to harvest low-grade thermal energy. J Membr Sci 2017;525:107–15.

[3] Long R, Li B, Liu Z, Liu W. Performance analysis of a thermally regenerative electrochemical cycle for harvesting waste heat. Energy 2015;87:463–9.

[4] Long R, Liu W. Efficiency and its bounds of minimally nonlinear irreversible heat engines at arbitrary power. Phys Rev E 2016;94(5–1):052114.

[5] Long R, Liu W. Ecological optimization and coefficient of performance bounds of general refrigerators. Phys A Stat Mech Appl 2016;443:14–21.

[6] Hasani M, Rahbar N. Application of thermoelectric cooler as a power generator in waste heat recovery from a PEM fuel cell – an experimental study. Int J Hydrogen Energy 2015;40(43):15040–51.

[7] Barelli L, Bidini G, Gallorini F, Ottaviano A. An energetic–exergetic analysis of a residential CHP system based on PEM fuel cell. Appl Energy 2011;88(12):4334–42.

[8] Zhao P, Wang J, Gao L, Dai Y. Parametric analysis of a hybrid power system using organic Rankine cycle to recover waste heat from proton exchange membrane fuel cell. Int J Hydrogen Energy 2012;37(4):3382–91.

[9] Arun Saco S, Thundil Karuppa Raj R, Karthikeyan P. A study on scaled up proton exchange membrane fuel cell with various flow channels for optimizing power output by effective water management using numerical technique. Energy 2016;113:558–73.

[10] Cappa F, Facci AL, Ubertini S. Proton exchange membrane fuel cell for cooperating households: a convenient combined heat and power solution for residential applications. Energy 2015;90:1229–38.

[11] Chen X, Chen L, Guo J, Chen J. An available method exploiting the waste heat in a proton exchange membrane fuel cell system. Int J Hydrogen Energy 2011;36(10):6099–104.

[12] Ramousse J, Lottin O, Didierjean S, Maillet D. Heat sources in proton exchange membrane (PEM) fuel cells. J Power Sources 2009;192(2):435–41.

[13] Cozzolino R, Cicconardi SP, Galloni E, Minutillo M, Perna A. Theoretical and experimental investigations on thermal management of a PEMFC stack. Int J Hydrogen Energy 2011;36(13):8030–7.

[14] Long R, Li B, Liu Z, Liu W. A hybrid system using a regenerative electrochemical cycle to harvest waste heat from the proton exchange membrane fuel cell. Energy 2015;93:2079–86.

[15] Arsalis A, Nielsen MP, Kær SK. Modeling and off-design performance of a 1kWe HT-PEMFC (high temperature-proton exchange membrane fuel cell)-based residential micro-CHP (combined-heat-and-power) system for Danish single-family households. Energy 2011;36(2):993–1002.

[16] Gandiglio M, Lanzini A, Santarelli M, Leone P. Design and optimization of a proton exchange membrane fuel cell CHP system for residential use. Energy Build 2014;69:381–93.

[17] Lokare OR, Tavakkoli S, Rodriguez G, Khanna V, Vidic RD. Integrating membrane distillation with waste heat from natural gas compressor stations for produced water treatment in Pennsylvania. Desalination 2017;413:144–53.

[18] Maheswari KS, Kalidasa Murugavel K, Esakkimuthu G. Thermal desalination using diesel engine exhaust waste heat — an experimental analysis. Desalination 2015;358:94–100.

[19] Qtaishat M, Matsuura T, Kruczek B, Khayet M. Heat and mass transfer analysis in direct contact membrane distillation. Desalination 2008;219(1–3):272–92.

[20] Shih H, Shih T. Utilization of waste heat in the desalination process. Desalination 2007;204(1–3):464–70.

[21] Zhou S, Guo Y, Mu X, Shen S. Effect of design parameters on thermodynamic losses of the heat transfer process in LT-MEE desalination plant. Desalination 2015;375:40–7.

[22] Choi S-H. Thermal type seawater desalination with barometric vacuum and solar energy. Energy 2017;141:1332–49.

[23] Hanshik C, Jeong H, Jeong K-W, Choi S-H. Improved productivity of the MSF (multi-stage flashing) desalination plant by increasing the TBT (top brine temperature). Energy 2016;107:683–92.

[24] Palenzuela P, Zaragoza G, Alarcón-Padilla D-C. Characterisation of the coupling of multi-effect distillation plants to concentrating solar power plants. Energy 2015;82:986–95.

[25] Li C, Goswami DY, Shapiro A, Stefanakos EK, Demirkaya G. A new combined power and desalination system driven by low grade heat for concentrated brine. Energy 2012;46(1):582–95.

[26] Bui VA, Vu LTT, Nguyen MH. Modelling the simultaneous heat and mass transfer of direct contact membrane distillation in hollow fibre modules. J Membr Sci 2010;353(1–2):85–93.

[27] Chen T-C, Ho C-D, Yeh H-M. Theoretical modeling and experimental analysis of direct contact membrane distillation. J Membr Sci 2009;330(1–2):279–87.

[28] Bui VA, Nguyen MH, Muller J. The energy challenge of direct contact membrane distillation in low temperature concentration. Asia Pac J Chem Eng 2007;2(5):400–6.

[29] Bouguecha ST, Aly SE, Al-Beirutty MH, Hamdi MM, Boubakri A. Solar driven DCMD: performance evaluation and thermal energy efficiency. Chem Eng Res Des 2015;100:331–40.

[30] Dow N, Gray S, Li J-d, Zhang J, Ostarcevic E, Liubinas A, et al. Pilot trial of membrane distillation driven by low grade waste heat: membrane fouling and energy assessment. Desalination 2016;391:30–42.

[31] Sun Z, Wang N, Bi Y, Srinivasan D. Parameter identification of PEMFC model based on hybrid adaptive differential evolution algorithm. Energy 2015;90:1334–41.

[32] Fathy A, Rezk H. Multi-verse optimizer for identifying the optimal parameters of PEMFC model. Energy 2018;143:634–44.

[33] Kayvani Fard A, Manawi YM, Rhadfi T, Mahmoud KA, Khraisheh M, Benyahia F. Synoptic analysis of direct contact membrane distillation

performance in Qatar: a case study. Desalination 2015;360:97–107.
[34] Guan G, Yang X, Wang R, Fane AG. Evaluation of heat utilization in membrane distillation desalination system integrated with heat recovery. Desalination 2015;366:80–93.
[35] Miansari M, Sedighi K, Amidpour M, Alizadeh E, Miansari M. Experimental and thermodynamic approach on proton exchange membrane fuel cell performance. J Power Sources 2009;190(2):356–61.
[36] Amphlett JC, Baumert RM, Mann RF, Peppley BA, Roberge PR, Harris TJ. Performance modeling of the Ballard Mark IV solid polymer electrolyte fuel cell I. Mechanistic model development. J Electrochem Soc 1995;142(1):1–8.
[37] Lin S, Yip NY, Elimelech M. Direct contact membrane distillation with heat recovery: thermodynamic insights from module scale modeling. J Membr Sci 2014;453:498–515.
[38] Ene S, Küçükoğlu İ, Aksoy A, Öztürk N. A genetic algorithm for minimizing energy consumption in warehouses. Energy 2016;114:973–80.
[39] Mo ZJ, Zhu XJ, Wei LY, Cao GY. Parameter optimization for a PEMFC model with a hybrid genetic algorithm. Int J Energy Res 2006;30(8):585–97.
[40] Lee S. Multi-parameter optimization of cold energy recovery in cascade Rankine cycle for LNG regasification using genetic algorithm. Energy 2017;118:776–82.
[41] Zheng N, Liu P, Shan F, Liu Z, Liu W. Sensitivity analysis and multi-objective optimization of a heat exchanger tube with conical strip vortex generators. Appl Therm Eng 2017;122:642–52.
[42] Long R, Li B, Liu Z, Liu W. Multi-objective optimization of a continuous thermally regenerative electrochemical cycle for waste heat recovery. Energy 2015;93:1022–9.